High Angle-of-Attack Calculations of the Subsonic Vortex Flow on Slender Bodies

D. Almosnino*
NASA Ames Research Center, Moffett Field, California

A nonlinear vortex-lattice method is used for the calculation of separated vortex flows over slender bodies at high incidence. Symmetric and asymmetric vortex flow cases are calculated showing good agreement with recently obtained experimental data for an ogive-cylinder body at high Reynolds numbers. The only input needed for these calculations is the positions of the separation lines on the body. Studies of some of the numerical aspects of this method are described and conclusions are implemented to improve the calculations.

Nomenclature

A = influence coefficient matrix
C_L = lift coefficient
C_m = pitching moment coefficient about nose tip
C_n = yawing moment coefficient about nose tip
C_N = normal force coefficient
C_p = pressure coefficient
C_Y = side force coefficient
D = maximum body diameter
F = fixed part of A
L = body length
M = Mach number
$\hat{n}$ = vector normal to surface
Nc = axial number of elemental panels
Ns = circumferential number of elemental panels
R = maximum radius of body
r = distance
Re_d = Reynolds number based on diameter
S_0 = potential sources strength vector
U = freestream velocity
u,v,w = velocity disturbance Cartesian components
$V(X_n)$ = variable part of A
x,y,z = Cartesian coordinates
X = potential vortices strength vector
α = angle of attack
β,γ = geometrical angles
Γ = vortex strength
Δx = vortex trajectory integration step size
θ = circumferential angle

Mathematical Symbol

$\| \|$ = norm of a matrix

Subscripts

0 = at $\alpha = 0$ deg
i = index
N = nose
n = iteration number

I. Introduction

THE increasing interest in high-angle-of-attack aerodynamics has heightened the need for computational tools suitable to predict the flowfield and the aerodynamic coefficients in this regime. Of particular interest and complexity are the symmetric and the asymmetric separated vortex flows which develop about slender bodies as the angle of attack is increased.[1] The viscous influence on the separation lines and the unknown three-dimensional (3D) shape of the vortex wake are some of the main flow features that must be modeled in the construction of a computational method to properly treat this problem.

Among the many potential flow methods developed in attempting to solve body vortex flows are early two-dimensional (2D) multivortex methods,[2-4] 2D time-stepping vortex models that include boundary-layer considerations,[5-8] and a quasi-3D potential flow method[9] that uses source and vortex elements. Linear, unseparated potential flow models, as well as purely viscous models, are not mentioned here. A survey of the various methods may also be found in Ref. 10. The potential flow methods are of special interest because of their ability to treat 3D body shapes and their separated vortex flows using a simple and relatively inexpensive model. However, the previously mentioned methods suffer from some limitations mainly concerning the treatment of the vortex wake formation and its interaction with the body. The first group of methods[2-4] cannot treat 3D flows and is limited to very slender bodies. The second group of computational methods[5-8] is time consuming and therefore expensive, and its separation prediction is not sufficiently accurate. Both the methods in this group and the method in Ref. 9 suffer from the dependency on too many semiempirical inputs and assumptions concerning the vortex wake and its separation. The steady, 3D nonlinear vortex-lattice method,[11,12] upon which the present method is based, eliminates many of these limitations by introducing a more consistent model, but it can treat only symmetrical flow cases. The present work extends the use of the last model to asymmetric, body-vortex flow cases, thus increasing the range of flow problems that can be investigated. In addition, an effort is made to improve the numerical procedure to accelerate the convergence of the iterative solution and to get a better rollup of the vortex lines representing the wake.

II. Present Method

General

The recently developed nonlinear vortex-lattice method[11,12] has been modified and improved to include asymmetric flow calculations. The basic mathematical model used for the calculations is similar to that used in Ref. 12, except that no symmetry condition is imposed on the body or on its vortex wake, and the calculation of the aerodynamic coefficients includes the static lateral coefficients C_y and C_n. The model (Figs. 1a-c) consists of potential-flow elements to describe the body in an inviscid flow. A discrete source distribution along the body axis approximately describes the thickness function

Presented as Paper 83-0035 at the AIAA 21st Aerospace Sciences Meeting, Reno, Nev., Jan. 10-13, 1983; received Feb. 3, 1983; revision received July 4, 1984. This paper is declared a work of the U.S. Government and therefore is in the public domain.

*NASA/NRC Research Associate. Member AIAA.

of the body at zero incidence (Fig. 1a), while a vortex-lattice system of elemental panels is imposed on the source flowfield to account for the angle-of-attack effect.[12] The vortex system is composed of horseshoe vortices that are distributed on the surface of the body (Fig. 1b). The head of each vortex lies in the surface; its trailing arms may either stay in the surface or leave it entirely to simulate the vortex separation (Fig. 1c). The shedding of trailing vortices is restricted to certain predetermined separation points. Either empirical data or calculated results may be used for this purpose; the former option is being used in this work as an external input. It is assumed that the separation is confined to a narrow region (line) on the surface as shown by empirical evidence,[13-20] and that the separated vortex sheet may then be treated by using potential flow elements.

Calculation Procedure

The calculation method is illustrated in Fig. 2. First, the source strengths at zero incidence, S_0, are determined from

$$A_0 S_0 = -\vec{U}\cdot\hat{n}_0 \tag{1}$$

where A_0 is an influence coefficient matrix that calculates the velocities induced by the axial sources of Fig. 1a, in this case of unit strength, at the control points on each elemental panel, normal to its surface. No net flow is allowed through the surface at these points, $\hat{n}_0$ being the vector of normals to the surface at the control points. The body is now positioned at the prescribed angle of attack and a second influence coefficient matrix A is calculated. This matrix computes the normal component of the velocity, induced by unit strength vortices located in the panels of Figs. 1b and 1c and by their wake, at the control point on each elemental panel. The strength X of the bound vortices can be calculated from

$$AX + A_0 S_0 = -\vec{U}\cdot\hat{n} \tag{2}$$

where $\hat{n}$ is the vector of the normals to the surface at the control points for the given angle of attack. The tangency boundary condition for the flow over the body surface is again used in Eq. (2). In the first iterative cycle, an initial guess has to be made as to the shape of the free vortex lines representing the wake downstream of the prescribed separation line. Each of the free vortex lines is constructed in the code out of a number of straight, finite-length segments between designated points. In the absence of any data about the shape of the wake, the calculation may be started from an unseparated, potential flow solution over a closed body. Since the form of the wake is not known a priori, the segmented vortex lines which represent the wake have to relax to their steady position in the flow by an iterative process. For that purpose, the downstream point of each segment is moved so that the segment is approximately aligned with the local flow direction to satisfy the boundary condition on the wake, as the wake is not allowed to support any forces. A Euler-type integration method is used for that purpose:

$$y_i^* = y_{i-1}^* + \left(\frac{v}{U+u}\right)_{i-1}^* \Delta x_i$$

$$z_i^* = z_{i-1}^* + \left(\frac{w}{U+u}\right)_{i-1}^* \Delta x_i \tag{3}$$

where y_i^* and z_i^* are the new coordinates of the downstream end of segment i, and are being calculated by using the new position of the downstream end point of segment $i-1$ found in the previous step. The asterisk denotes that the locations of the newly calculated vortex trajectories and the velocities they induce take part in the relaxation process to enhance the convergence of the wake. The velocity disturbance components (u,v,w) at each point are obtained using the Biot-

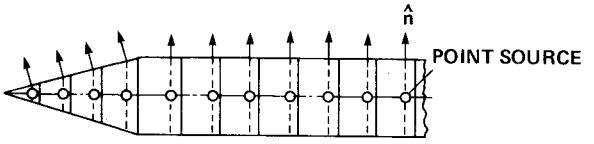

a) Typical arrangement of point sources on body axis for zero angle-of-attack solution (for axisymmetric bodies only).

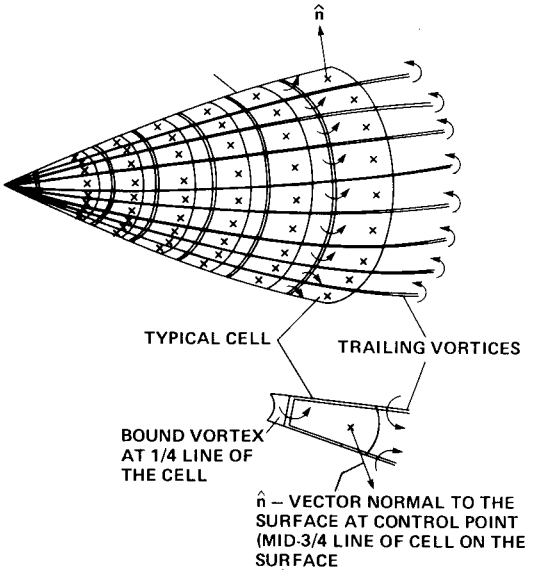

b) Part of a body, divided into elemental panels.

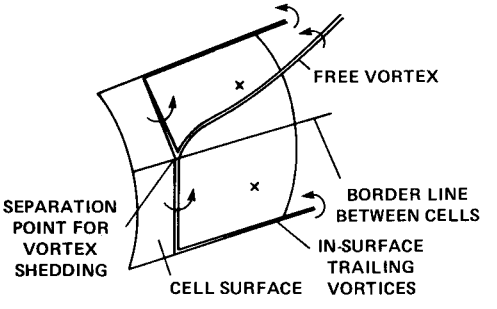

c) Model for separating vortices from the surface of the body.

Fig. 1 Vortex model including separation, present method.

Savart law for the velocity induced by a vortex segment on a given point. Contrary to previous practice,[12] no symmetry condition is imposed on the free vortices or on the body in the present method, and the integration involves all vortices from both sides of the body. Other integration methods, such as second-order Runge-Kutta, have been tried in the present work, but their effect on the results was too small to justify the increased cost. The relaxation of the wake is usually carried out only once in every main iteration for the strength X. An inner iterative cycle (Fig. 2) is optional, but is not necessary in most cases. Note that any geometrical change occurring in the shape of the vortex trajectories during the relaxation cycle also produces a slight change in the local flow direction at previously calculated points of the wake. The inner cycle repeats the relaxation procedure over the wake for a specified number of times to correct the error accumulated in the local inclination of each vortex segment and realign it with the local flow direction. Upon completing the inner loop, the influence-coefficient matrix is updated to account for the new geometry of the wake, and the whole process is repeated until convergence of the bound vortices

strength and the free vortices trajectories is achieved (Fig. 2). The main iterative cycle can be written as[12]

$$[F+V(X_n)]X_{n+1}=-(\vec{U}\cdot\hat{n}-\vec{U}\cdot\hat{n}_0) \tag{4}$$

where X_n and X_{n+1} are the solution vectors for the bound vortices strength in the corresponding iterative cycles n and $n+1$, and the influence coefficient matrix A is divided into a fixed part F that depends on the body geometry only and a variable part $V(X_n)$ that depends on the relaxed wake geometry in iteration cycle n. To save computer time, matrix F is computed only once for a given configuration and mesh, because the bound vortex segments do not change their positions relative to the control points. Once convergence is achieved, the pressure distribution and the aerodynamic coefficients are calculated. The cost involving the addition to the other half of the body and the corresponding part of the wake is substantial. The CPU time is roughly quadrupled when compared with the symmetrical code for an equal number of iterations with the same mesh density. There is also a substantial increase in required core memory that is four times as large for the same comparison, but this problem is less acute because inactive large arrays are written in a temporary file.

Numerical Considerations

While the method was being modified to accommodate asymmetry, various numerical considerations that were developed[12] were also incorporated here. In Ref. 12, a simple analysis of Eq. (4) shows that if a solution exists, and if the initial guess for the wake is close enough to its final shape, then the sufficient condition for the convergence of the main iterative process is that for each iteration n,

$$\|[F+V(X_n)]^{-1}\cdot X_n\cdot(\partial V/\partial X)_n\|<1 \tag{5}$$

provided that X is within a certain radius (not known a priori) from the converged solution. Simple conclusions[12] drawn from examining the meaning of Eq. (5) are implemented in the present modified method to accelerate the convergence rate of the solution:

1) The initial shape of the vortex filaments required to start the iterative process may now be specified using previously calculated data at a lower angle of attack. This allows for a gradual buildup of a solution from an initially low incidence to a higher one, improving the overall convergence rate. This procedure leads to lower values of $(\partial V/\partial X)_n$ in Eq. (5), and it is found that the number of main iteration cycles needed for convergence at high incidence is typically about half of that required when solving the same problem with an unseparated flow as an initial guess. Some high-incidence cases that could not converge before can now do so using this procedure.

2) The inverse of the influence coefficients matrix, $[F+V(X_n)]^{-1}$, plays an important role in determining the convergence rate of the method. F is never ill-conditioned because of the geometric structure of the vortex lattice; however, $V(X_n)$ depends on the geometry of the wake and may cause numerical problems. For example, this happens when a free vortex passes too close to a control point. The condition for convergence [Eq. (5)] calls for a strengthening of the dominance of the main diagonal of F to improve the convergence rate. Increasing the number of cells in the lattice may achieve this goal[12] since the main diagonal of F is strengthened when the distance between the bound vortex and the control point decreases, but such an increase is very costly and may also lead to other numerical problems involving the solution of very large systems of linear equations. Another way to strengthen the main diagonal of F is to move the control points slightly closer to the heads of the corresponding bound vortices, thus increasing the self-induced velocity of each elemental panel. A preliminary investigation of this idea revealed that moving the control points in this manner helped convergence, but that the overall aerodynamic coefficients were also affected. This method was used to achieve convergence under severe conditions of high incidence ($\alpha>20$ deg), but the sensitivity of the solution to the geometrical structure of the cell requires further investigation.

3) To prevent the generation of exaggerated induced velocities due to the singularity of potential flow vortex elements, all vortex-lattice methods use some kind of a "cutoff distance" that puts a limit to the influence of such vortex elements. In the present method, the cutoff distance is used to determine the distance from a vortex segment, inside which a solid-body rotation is assumed for the influencing

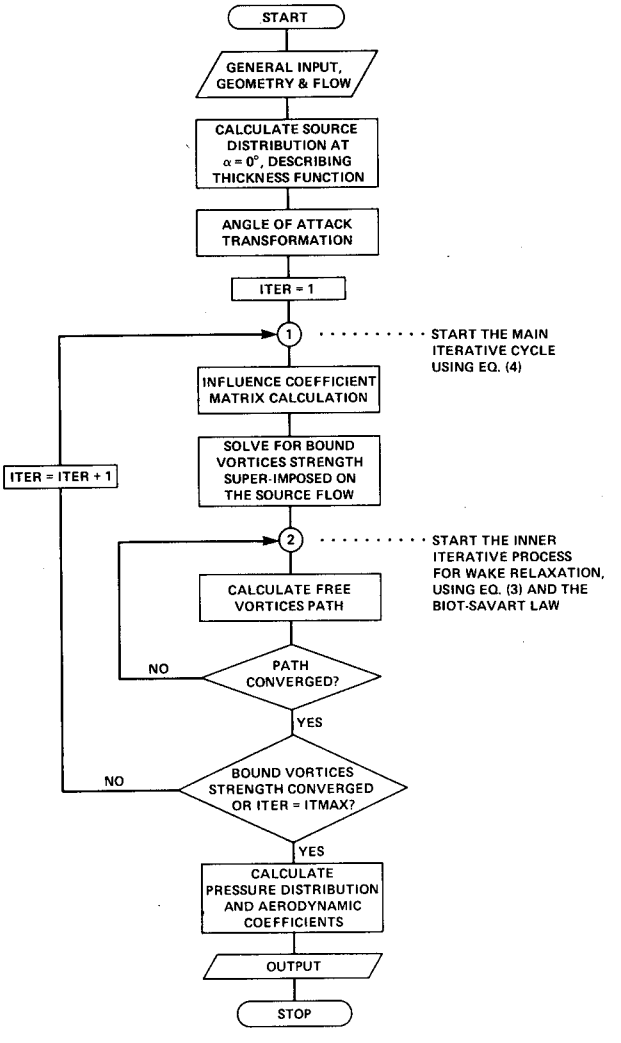

Fig. 2 Flowchart of the calculation scheme.

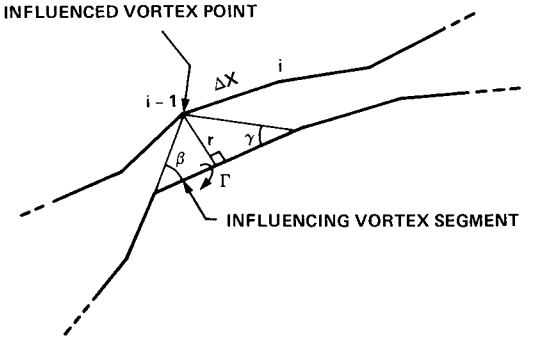

Fig. 3 Geometry used for cutoff distance evaluation.

vortex. The numerical results and the convergence rate are influenced by this parameter, which introduces numerical damping into the calculations. Experiments with this parameter in the present work showed, as expected,[21] that the main effect of a cutoff distance is on the wake rollup. A large cutoff distance prevents a good rollup, whereas a small one may cause divergence of the vortex filaments or a nonphysical wake form where the vortex sheet formed by the filaments cuts through itself. A small cutoff distance may also generate large local pressure variations on the surface of the body in the proximity of a free vortex. The problems associated with a small cutoff distance usually give rise to longer computation times. In view of these observations, which are well known to users of discrete-vortex wake-representation methods, an attempt was made to define a criterion for an optimum cutoff distance by studying its effect on the rollup iterative relaxation process of Eq. (3). Given a single vortex segment of strength Γ that induces a velocity on another vortex segment of length Δx (Fig. 3), it can be shown (with some simplifying assumptions) that the maximal induced angular velocity of point i relative to the inducing vortex segment is obtained in the consecutive integration step of Eq. (3), when the distance between the segment and point $i-1$ is given approximately by

$$r^* = \left[\frac{\Gamma \cdot \Delta x(\cos\beta + \cos\gamma)}{4\pi U}\right]^{1/2} \tag{6}$$

This maximum angular velocity enhances the rapid and proper rollup of the vortex lines. For a cutoff distance that is larger than r^*, the angular velocity is too low causing a weak rollup. For any cutoff distance smaller than r^*, the angular velocity is lower than the maximum, but the induced linear velocity increases very rapidly so that point i of the segment would be displaced by an excessive distance when using the integration given by Eq. (3). This would prevent a good rollup in the following steps and may even lead to the divergence of the relaxation process. Note that when r^* is used as a cutoff distance, it is locally dependent on two main features of the vortex model, namely the strength of the influencing vortex and the lengths of both segments (or the integration step). This makes the cutoff criterion sensitive to the local conditions at each step of the relaxation process, as opposed to an arbitrary choice of a single-valued cutoff distance for the whole flowfield. Although some additional computational effort is required, the cost of using this parameter is not substantial (estimated additional 5%) because the required quantities already have been calculated by the subroutine that computes the induced velocities, and because it produces an accelerated convergence. The implementation of Eq. (6) for a cutoff criterion yields better convergence than a fixed cutoff distance case (10-20% fewer iterations) and yields a better rollup of the wake (by qualitative comparison only), and in some cases it makes the difference between unconverged and converged solutions.

The various improvements in the calculation procedure, together with some other technical improvements, have significantly increased the efficiency of the computer code. In particular, computing time and active memory core have been reduced, compared with previously reported data,[11,12] by at least 50% (an approximate estimate of the actual saving for the same computer, when computing identical cases).

III. Results

The modified code was tested on an ogive-cylinder body with a nose fineness ratio of $L_N/D=3.5$ and an overall ratio of $L/D=7.5$. Detailed pressure data for this body at low speed ($M=0.27$), Reynolds numbers from $Re_d=0.2\times10^6$ to 3.9×10^6, and for angles of attack ranging up to 90 deg were published by Lamont[22] (also unpublished data, 1980). These data, together with some qualitative information from oil-flow visualization tests[23] at lower Reynolds numbers, give indications of the positions of the separation lines on the body. The separation lines are specified for the computer code as part of the input. Only the high Reynolds number data are used in the present calculation because the separation lines can then be easily determined from the pressure data.

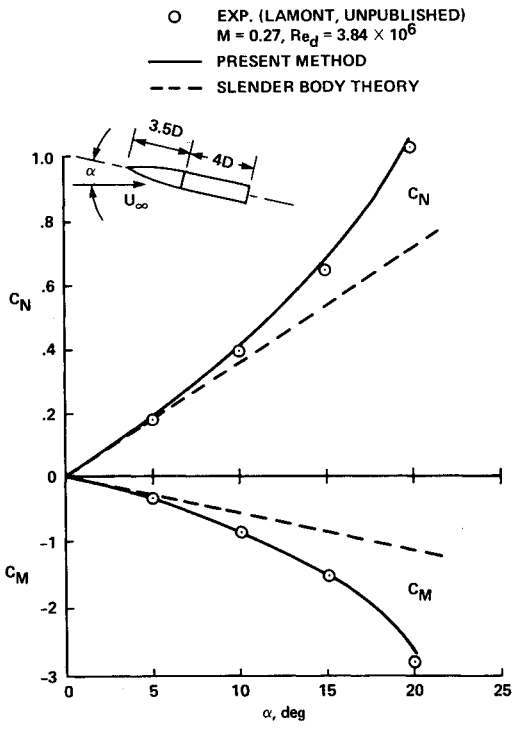

Fig. 4 Normal force and pitching moment coefficients on an ogive-cylinder body in subsonic flow.

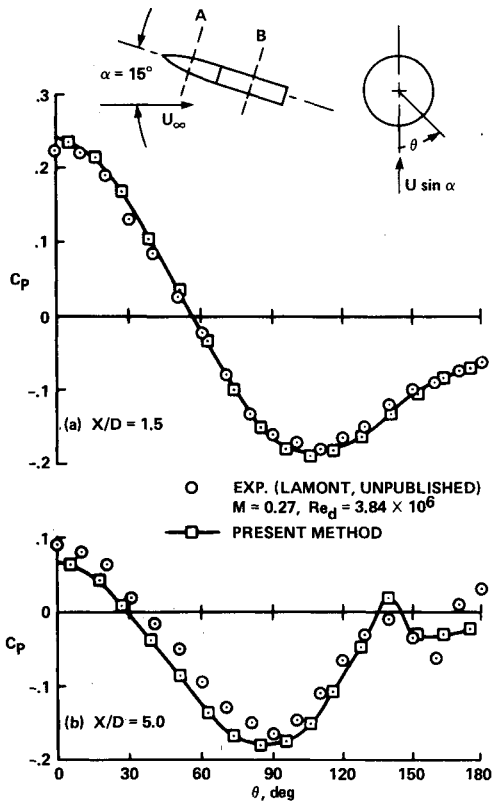

Fig. 5 Circumferential surface pressure distributions on an ogive-cylinder body in subsonic flow.

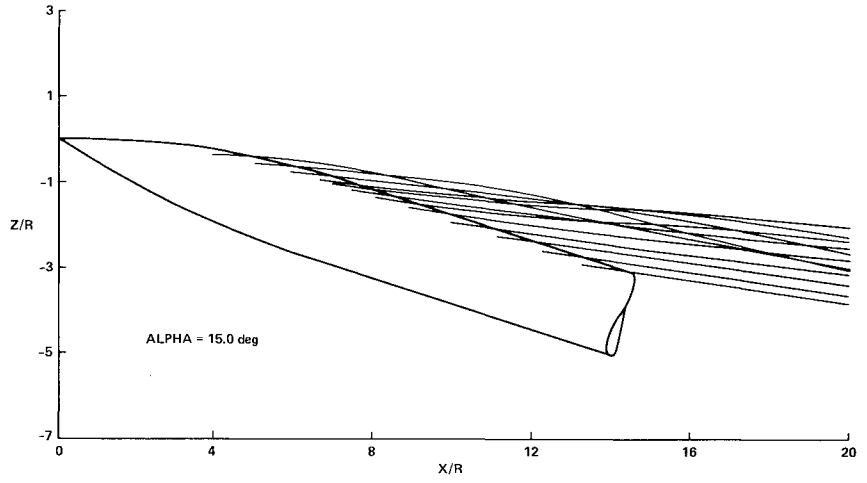

a) Side view of body vortices, wind axes.

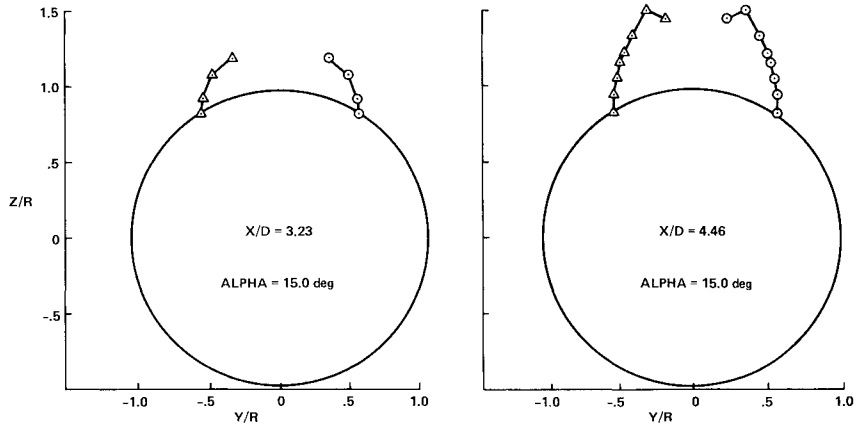

b) Cross-flow view of vortex wake, body axes.

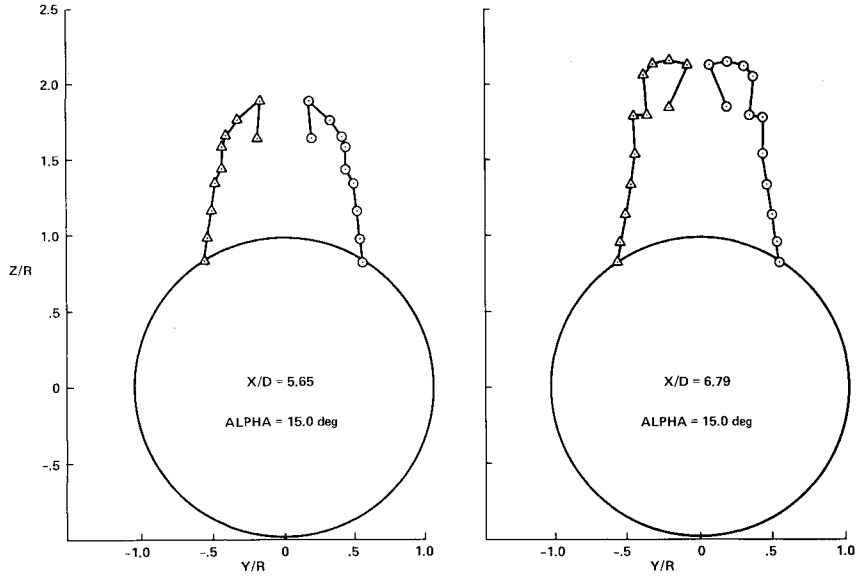

c) Cross view of vortex wake, concluded.

Fig. 6 An example of the calculated vortex rollup.

Symmetric Flow Calculations

The modified method was first checked out in symmetric flow cases to evaluate the numerical improvements. Good agreement was obtained for the normal force and the pitching moment coefficients for angles of attack to $\alpha = 25$ deg (Fig. 4). Some examples of the surface pressure distributions at $\alpha = 15$ deg are shown in Fig. 5. The agreement between the calculated results and the experimental data is good for the nose data. The calculated pressures on the cylindrical part of the body show a correct qualitative sensitivity to the presence of the vortex wake in spite of a coarse mesh and a possible secondary separation in the real flow. The description of the wake development, obtained when the separation of multiple vortex filaments along the body length was permitted, was much better than the one reported in Ref. 12, where the number of filaments is small because of computer limitations. As a result, there was a substantial improvement in the leeside pressure distribution on the aft portion of the body and consequently also in the pitching moment coefficient that was erroneous in Ref. 12. (A direct comparison is not

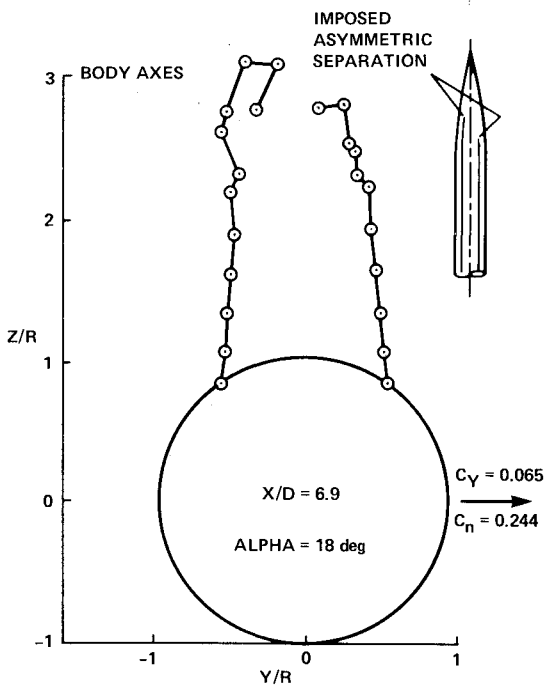

Fig. 7 Cross-flow view of vortex, asymmetric case.

shown here since the cases treated were different.) The discrepancy between the calculated levels of the pressures and the experimental data on the windward side of the cylinder (Fig. 5) may be due in part to the effect of the support system used in the experiment,[24,25] an effect that can be found even in Lamont's zero incidence data (1980, unpublished). An example of the calculated vortex rollup is presented in Fig. 6, using 12 vortices to represent the vortex wake. The vortex flow in this figure is in good qualitative agreement with various flow visualization pictures taken on ogive-cylinder bodies at similar angles of attack (e.g., Fiechter, 1969, in Ref. 26) and is an improvement over the corresponding case in Ref. 12.

Asymmetric Flow Calculations

The present vortex-lattice method handles the entire body and flowfield so that asymmetric flows can be simulated. The stability of this method in the asymmetric mode was first checked by creating a slight disturbance in the shape of the vortex lines representing the wake at $\alpha = 18$ deg, while keeping the separation points symmetric. It was found that the solution converged to the symmetric one after a few iterations.

Next, asymmetry between the left and the right separation lines on the body was imposed. The asymmetry between the two separation lines was obtained by moving the separation line on the right side of the body slightly downstream, resulting in an asymmetric flow solution (Fig. 7). The asymmetric flow influenced the pressure distribution and caused the appearance of a steady side force and yawing moment. The asymmetric pressure distribution at $\alpha = 25$ deg is presented in Fig. 8. Of particular interest is the effect of the asymmetry on the pressure distributions along the sides of the body ($\theta = \pm 90$ deg) due to the influences of the leeside asymmetric vortex flow that is fed through the flowfield to the windside part of the body. This asymmetry is the main cause for the existence of the side force, while the asymmetry of the pressure distribution due to the effect of the primary vortices on the leeside of the body contributes much less to it. The side force and yawing moment coefficients are depicted for a range of angles of attack in Fig. 9. Although these results are correctly indicative of the effects of asymmetric shedding, they cannot be directly compared with La-

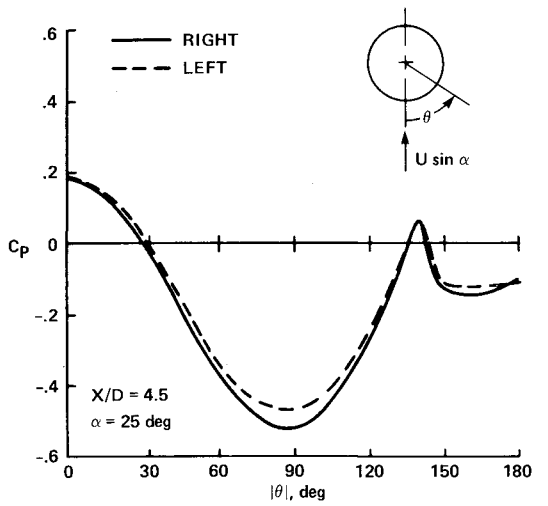

Fig. 8 Circumferential surface pressure coefficient due to asymmetry in separation.

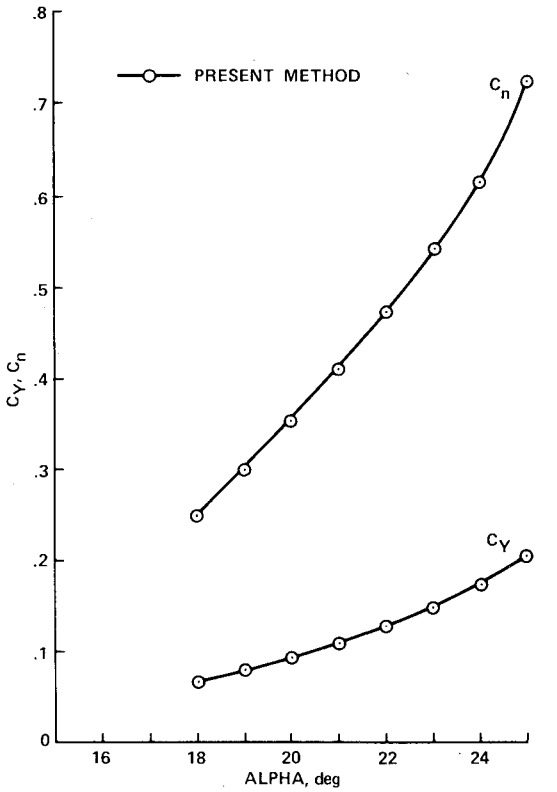

Fig. 9 Side force and yawing moment coefficients due to asymmetry in separation.

mont's experimental data (1980, unpublished). Lamont found the onset on asymmetry for this body at about 18 deg and different values for the side force and yawing moment coefficients, but he did not present detailed experimental data concerning the position and the shape of the separation lines at the various angles of attack. These were also highly dependent on the roll angle of the body and on the Reynolds number. The lack of such data rules out a direct comparison. The nonphysical asymmetry imposed in this computation was used to illustrate the potential of the modified code in asymmetric cases. There was no experimental guidance in choosing the positions of the separation lines (Fig. 7) when the angle of attack increased. Figure 9 therefore represents only a qualitative effect of increasing angle of attack on the lateral aerodynamic coefficients. In spite of this, the magnitude of the calculated side force and yawing moment is found to be within the large scatter of ex-

perimental results for different roll angles. This may be explained by the fact that the asymmetry actually starts to grow gradually from a slight disturbance in the symmetry of the separation lines, so that the order of magnitude of the resulting lateral force is similar in both cases.

IV. Summary

The nonlinear vortex-lattice method of Ref. 12 has been extended to calculate asymmetric flows over slender bodies as follows:

1) The method has been extended to include the calculation of asymmetric flow on the body, using externally specified data for the asymmetric separation lines.

2) The initial form of the vortex filaments at the beginning of the iterative process may be specified using data previously calculated at a lower angle of attack. This allows for a gradual buildup of a solution from an initial low incidence to the higher one, improving the convergence rate and saving computer resources.

3) The use of a new, variable cutoff-distance criterion improves the rollup of the wake and the relaxation process.

4) Computing time and active memory core have been substantially reduced compared with previously reported data.[11,12]

The main input needed to obtain results that can be compared with experimental data is the positions of the separation lines. When provided by this input the method can be effectively used to calculate steady symmetric and asymmetric subsonic separated vortex flows over three-dimensional bodies. More detailed studies of the numerical characteristics of this method will be published in a later paper. It is also recommended that further investigations be made on the effect of the experimental support system on the body at all angles of attack, and that the feasibility of allowing a viscous calculation to interact with the inviscid vortex code in order to obtain independent data on the separation positions be checked. Some recent attempts to calculate such an interaction look promising.[27]

Acknowledgment

The author would like to thank Dr. L. B. Schiff, Research Scientist at NASA Ames Research Center, for his helpful comments throughout the research.

References

[1]Hunt, B. L., "Asymmetric Vortex Forces and Wakes on Slender Bodies," AIAA Paper 82-1336, Aug. 1982.

[2]Angelucci, S. B., "A Multi Vortex Method for Axisymmetric Bodies at Angle of Attack," *Journal of Aircraft*, Vol. 8, Dec. 1971, pp. 959-966.

[3]Angelucci, S. B., "Multi Vortex Model for Bodies of Arbitrary Cross Sectional Shapes," AIAA Paper 73-104, Jan. 1973.

[4]Fidler, J. E., "Approximate Method for Estimating Wake Vortex Strength," *AIAA Journal*, Vol. 12, May 1974, pp. 633-635.

[5]Marshal, F. J. and Deffenbaugh, F. D., "Separated Flow over Bodies of Revolution Using an Unsteady Discrete Vorticity Cross Wake," NASA CR 2414, June 1974.

[6]Wardlaw, A. B. Jr., "Multivortex Model of Asymmetric Shedding on Slender Bodies at High Angles of Attack," AIAA Paper 75-123, Jan. 1975.

[7]Deffenbaugh, F. D. and Koerner, W. G., "Asymmetric Vortex Wake Development on Missiles at High Angles of Attack," *Journal of Spacecraft and Rockets*, Vol. 14, March 1977, pp. 155-162.

[8]Deffenbaugh, F. D. and Shivananda, T. P., "Discrete Vortex Modeling of Separated Flow Phenomena," TRW Systems and Energy Inc., Redondo Beach, Calif., Rept. 33945-6001-ut-00, Aug. 1980.

[9]Sheffield, S. J. and Deffenbaugh, F. D., "A 3-D Vortex Wake Model for Missiles at High Angles of Attack," NASA CR 3208, Jan. 1980.

[10]Nielsen, J. N., "Nonlinearities in Missile Aerodynamics," AIAA Paper 78-20, Jan. 1978.

[11]Rom, J., Almosnino, D., and Gordon, R., "Method for the Calculation of the Non-Linear Aerodynamic Characteristics of Thick Wings and Bodies Including Symmetric Vortex Separation in Subsonic Flows," Dept. of Aeronautical Engineering, Technion, Haifa, Israel, TAE Rept. 437, Jan. 1981.

[12]Almosnino, D. and Rom, J., "Calculation of Symmetric Vortex Separation Affecting Subsonic Bodies at High Incidence," *AIAA Journal*, Vol. 21, March 1983, pp. 398-406.

[13]Mendenhall, M. R. and Nielsen, J. N., "Effect of Symmetrical Vortex Shedding on the Longitudinal Aerodynamic Characteristics of Wing-Body-Tail Combinations," NASA CR-2473, 1975.

[14]Clark, W. H., Peoples, J. R., and Briggs, M. M., "Occurrence and Inhibition of Large Yawing Moments during High Incidence Flight of Slender Missile Configurations," AIAA Paper 72-968, Sept. 1972.

[15]Peake, D. J., Owen, K. F., and Higuchi, H., "Symmetrical and Asymmetrical Separations about a Yawed Cone," AGARD CP 247, *High Angle of Attack Aerodynamics*, Oct. 1978, pp. 16-1-16-27.

[16]Clark, W. C. and Nelson, R. C., "Body Vortex Formation on Missiles at High Angles of Attack," AIAA Paper 76-65, Jan. 1976.

[17]Thomson, K. D. and Morrison, D. F., "The Spacing Position and Strength of Vortices in the Wake of Slender Cylindrical Bodies at Large Incidence," Weapon Research Establishment, Salisbury, South Australia, Tech. Rept. NSA 25, June 1969; also, *Journal of Fluid Mechanics*, Vol. 50, Pt. 4, Dec. 1971, pp. 751-783.

[18]Krouse, J. R., "Induced Side Forces on Slender Bodies at Angles of Attack and Mach Numbers of 0.55-0.80," Naval Ship Research and Development Center Rept. AL-79, Washington, D.C., May 1971.

[19]Pick, G. S., "Investigation of Side Forces on Ogive Cylinder Bodies at High Angles of Attack in the $M=0.5$ to 1.1 Range," AIAA Paper 71-570, June 1971.

[20]Clark, W. H., "Body Vortex Formation on Missiles in Compressible Flows," AIAA Paper 77-1154, Aug. 1977.

[21]Rom, J. and Zorea, C., "The Calculation of the Lift Distribution and the Near Vortex Wake behind High and Low Aspect Ratio Wings in Subsonic Flow," TAE Rept. 168, Dept. of Aeronautical Engineering, Technion, Haifa, Israel, Jan. 1973.

[22]Lamont, P. J., "The Complex Asymmetric Flow over a 3.5D Ogive Nose and Cylindrical Afterbody at High Angles of Attack," AIAA Paper 82-0053, Jan. 1982.

[23]Keener, E. R., "Oil-Flow Separation Patterns on an Ogive Forebody," NASA TM 81314, Oct. 1981.

[24]West, G. S. and Apelt, C. J., "The Effects of Tunnel Blockage and Aspect Ratio on the Mean Flow Past a Circular Cylinder with Reynolds Numbers between 10^4 and 10^5," *Journal of Fluid Mechanics*, Vol. 114, Jan. 1982, pp. 361-377.

[25]Lamont, P. J., "Pressure around an Inclined Ogive-Cylinder with Laminar, Transitional, or Turbulent Separation," *AIAA Journal*, Vol. 20, Nov. 1982, pp. 1492-1499.

[26]Van Dyke, M., *An Album of Fluid Motion*, 1st ed., The Parabolic Press, Stanford, Calif., 1982, p. 52.

[27]Chien, K. Y., Van Tuyl, A. H., and Hsieh, T., "Prediction of Flowfields about Bodies of Revolution at Large Incidence," AIAA Paper 84-0506, Jan. 1984.